Measurement Science and Technology

100 year anniversary
Measurement Science and Technology

PAPER

A fast and remote magnetonanothermometry for a liquid environment

To cite this article: Le He *et al* 2016 *Meas. Sci. Technol.* **27** 025901

IOP Publishing Measurement Science and Technology
Meas. Sci. Technol. 27 (2016) 025901 (6pp) doi:10.1088/0957-0233/27/2/025901

A fast and remote magnetonanothermometry for a liquid environment

Le He[1,2], Wenzhong Liu[2], Qingguo Xie[1], Shiqiang Pi[2] and P C Morais[2,3]

[1] Wuhan National Laboratory for Optoelectronics, Huazhong University of Science and Technology, Wuhan 430074, People's Republic of China
[2] School of Automation, Huazhong University of Science and Technology, Wuhan 430074, People's Republic of China
[3] Universidade de Brasília, Instituto de Física, Brasília DF 70910-900, Brazil

E-mail: lwz7410@hust.edu.cn

Received 7 August 2015, revised 2 November 2015
Accepted for publication 16 November 2015
Published 23 December 2015

Abstract

This study reports on a new approach for remote nanothermometry with short response time (milliseconds) aiming to operate in liquid media using AC susceptibility components of a suspended magnetic nanoparticle subjected to the Brownian relaxation mechanism. A simple, low cost, and accurate system was designed to measure AC susceptibility using an AC magnetic field at small amplitude (6 Oe) and frequency range (5 kHz) superimposed on a weak DC magnetic field (up to 30 Oe). A model based on the AC susceptibility of magnetic nanoparticles (30 nm average diameter) was constructed to describe the temperature measurement sensitivity of the dominated Brownian relaxation time. A new approach for remote nanothermometry was achieved with measured AC susceptibility by the designed system and the proposed model. Our experimental results show that our magnetonanothermometer allows temperature errors lower than 0.3 K with standard deviations lower than 0.1 K in the temperature range from 310 to 320 K.

Keywords: magnetonanothermometry, magnetic nanoparticle, AC susceptibility, Brownian relaxation mechanism, magnetic fluid

(Some figures may appear in colour only in the online journal)

1. Introduction

The application of magnetic nanoparticles (MNPs) in biomedical and biological research has attracted more and more attention, such as intra–extracellular magnetohyperthermia [1, 2], drug/gene delivery [3, 4], and cell physiology [5]. Under an AC magnetic field, MNPs were implemented for heating tumor tissue to a certain temperature range for cancer thermotherapy [6]. Loaded with a drug/gene, MNPs were used as carriers for drug/gene delivery [3]. The study of magnetic relaxation mechanisms on MNPs injected into live cells under an applied magnetic field has significant implications for intracellular hyperthermia [2, 7]. In the stated applications above, *in situ* temperature measurement plays a key role in the access of temperature-controlled intra–extracellular hyperthermia and drug/gene delivery. Therefore, it is of great interest and significance to study magnetonanothermometry for potential applications in biomedical and biological applications.

Recent reports have been focused on different approaches for remote temperature measurement using the properties of MNPs to probe temperature [8–13]. The majority of the reported methods [9–13] used the first-order Langevin function to describe static magnetic properties of MNPs. Weaver *et al* reported a magnetic nanothermometer using the ratio of the fifth to the third harmonics under an AC field [8, 9]. Zhong *et al* recently reported on a remote nanothermometer using the magnetization of MNPs as the thermometric property with an accuracy of 0.06 K under DC plus AC applied fields, operating at low frequencies (192 Hz) with a response time of 8 s [13].

However, the dynamic properties of MNPs have yet to be clearly explored for remote magnetonanothermometry,

despite their possible impacts when probing temperature within biological liquid media. In contrast to temperature measurement at low frequency, a shorter response time can be achieved at higher frequencies, which can be improved from seconds [10, 13] to milliseconds. When subjected to AC magnetic fields, MNPs exhibit relaxation behavior of magnetic moment, including Brownian and/or Néel relaxation mechanisms. The Brownian mechanism presents smooth temperature dependence, whereas the Néel mechanism shows a highly nonlinear dependence on temperature. Moreover, because of the relationship between relaxation time and particle size, and the influence of both relaxation mechanisms in defining the effective relaxation time optimal operation of MNPs as the nanothermometer relies on the appropriate selection of parameters that are intrinsic (MNP characteristics) as well as extrinsic (e.g. frequency range, field strength) [14]. Therefore, if MNPs are meant to be suspended in a liquid medium to work as nanothermometer combinations of higher excitation frequency (kHz region) and large monodomain particle size (above 25 nm) they would provide improved operational conditions, because the Brownian relaxation mechanism would be dominant [15].

The present study explores this particular scenario (Brownian relaxation behavior) and introduces a new experimental set up and the appropriate approach, involving real and imaginary components of the magnetic susceptibility of MNPs, to measure the temperature of a liquid medium. The introduced nanothermometer comprises a 30 nm average diameter MNP suspended as a commercial magnetic fluid (MF) sample and subjected to a combination of low amplitude (below 10 Oe) AC magnetic field (H_{AC}) in the kilohertz region superimposed on a weak (below 30 Oe) DC magnetic field (H_{DC}).

2. Methods

The magnetic response of an ensemble of single domain MNPs suspended in a liquid medium while subjected to a time (t)-dependent magnetic field (H) is accounted for by complex susceptibility, $\chi = \chi' - \mathrm{i}\chi''$, where χ' is in-phase (real) component and χ'' is the out-of-phase (imaginary) component. The solution of the relaxation equation of nanoparticle magnetization, $M(t)$, yields the complex susceptibility, $\chi = \chi_0/(1 + \mathrm{i}\omega\tau)$, from which real and imaginary components can be extracted [15]:

$$\chi' = \frac{1}{1+(\omega\tau)^2}\chi_0 \text{ and } \chi'' = \frac{\omega\tau}{1+(\omega\tau)^2}\chi_0 \qquad (1)$$

where χ_0 is the initial susceptibility, ω is the angular frequency of the time-dependent field, and τ is the effective relaxation time. With measured χ' and χ'', the effective relaxation time can be expressed as:

$$\tau = \frac{\chi''}{\omega\chi'} \qquad (2)$$

The effective relaxation time in equation (2) includes two components: The Brownian and the Néel relaxation times

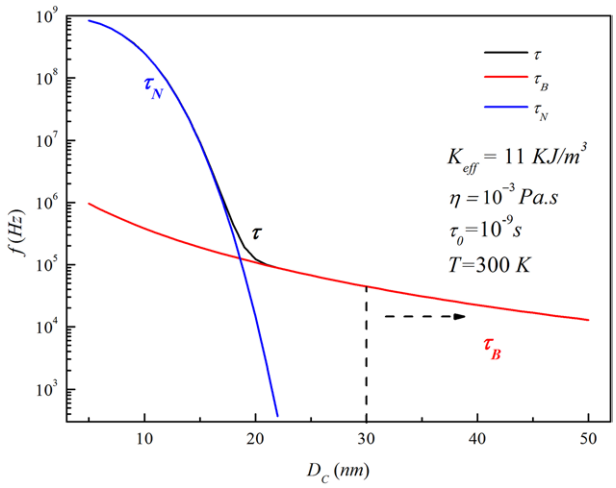

Figure 1. Simulation of the relaxation mechanisms of the magnetic moment of MNPs.

represented by τ_B and τ_N, respectively. Then, generally speaking, $1/\tau = 1/\tau_B + 1/\tau_N$ follows [15]. Figure 1 shows the simulation mechanisms of the magnetic moment of MNPs. Néel relaxation is dominant in the case of nanoparticles smaller than 15 nm, whereas Brownian relaxation is dominant in the case of nanoparticles larger than 25 nm. In this study, MNPs with an average size of 30 nm were chosen for the experiments, meaning that Brownian relaxation dominates and τ consequently approximately equals τ_B.

Furthermore, the Brownian relaxation time of MNPs suspended within a liquid medium can be assessed using a static approach, as described in the literature [16]:

$$\tau_B = \tau_B(0)\frac{\xi}{L(\xi)}\frac{\mathrm{d}L(\xi)}{\mathrm{d}\xi} = \tau_B(0)\frac{\xi}{L(\xi)}[1 - \coth^2(\xi) + \xi^{-2}] \qquad (3)$$

where $\tau_B(0) = \pi\eta D_H^3/(2kT)$ is the Brownian relaxation time at a zero-dc magnetic field, η is the liquid medium's viscosity, D_H is the MNP's hydrodynamic diameter, kT is the Boltzmann term, $L(\xi) = \coth(\xi) - 1/\xi$ is the first-order Langevin function, and $\xi = mH_{DC}/(kT)$ (m is the MNP's magnetic moment).

Under weak applied fields, the right-hand side of equation (3) can be approximated by:

$$\tau_B \cong \tau_B(0)[1 - (2/15)\xi^2 + (26/1575)\xi^4 + o(\xi^6)] \qquad (4)$$

The result can finally be expressed in terms of a DC applied field (H_{DC}) combining with equation (2) by selecting the appropriate particle size of 30 nm, inducing that effective relaxation time τ approximately equals τ_B:

$$\tau \cong \tau_B \cong (A_1/T) - (A_2/T)(H_{DC}/T)^2 + (A_3/T)(H_{DC}/T)^4 \qquad (5)$$

where $A_1 = \pi\eta D_H^3/(2k)$, $A_2 = \pi\eta m^2 D_H^3/(15k^3)$, and $A_3 = 13\pi\eta m^4 D_H^3/(1575k^5)$. Equation (5) reveals the temperature sensitivity of the relaxation time, which has the potential for nanothermometry. The two approaches of calculating the emphasized relaxation time, represented by equations (2) and (4), can be combined to assess the temperature of a liquid medium in which the MNP is suspended.

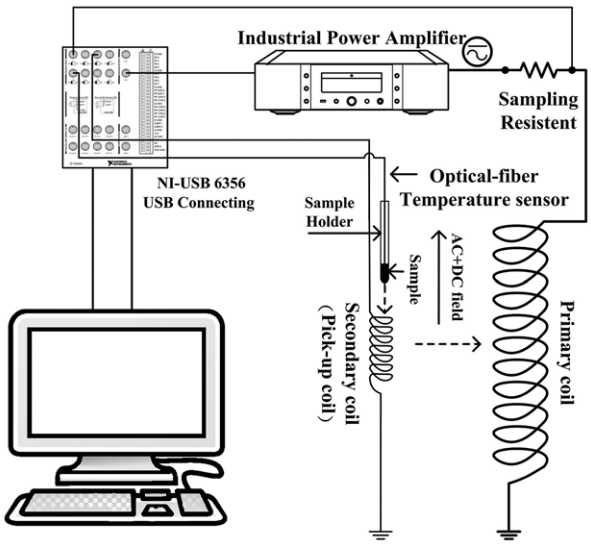

Figure 2. Schematic representation of the AC susceptibility (χ'' and χ') measuring system.

3. Magnetic nanoparticle susceptometer design

In the present study the relaxation time is experimentally obtained via equation (2) by measuring both out-of-phase (χ'') and in-phase (χ') components of the complex susceptibility using a simple, low cost, and precise experimental set up schematically presented in figure 2.

The diagram of the proposed instrument (see figure 2) includes a secondary coil axially inserted within a primary coil. In the figure diagram (see figure 2) the secondary coil is displaced from the primary coil for a better view. The data acquisition card (NI USB-6356) is computer controlled and used to generate AC and DC signals, as well as data acquisition. The AC and DC signals are amplified by a high-precision industrial power amplifier (AE7224, AE Techron, Inc) to drive the primary coil for producing time-dependent fields, $H(t) = H_{DC} + H_{AC}(t)$. Then, the data acquisition card collects voltage signals from both the secondary coil and the optical-fiber temperature sensor (reference) with all the data processed within the Labview® platform.

To assess the relaxation time using equation (2) the susceptibility components (χ'' and χ') are obtained by recording the voltage from the secondary coil (see figure 2) without the MF sample within the coil, $V_1(t)$, and after inserting the MF into the coil, $V_2(t)$. The recorded signals from time-dependent applied fields are described by:

$$V_i(t) = \sum_{j=1}^{n} -\mathrm{d}\Phi_{ij}/\mathrm{d}t = \sum_{j=1}^{n} -s_j \mathrm{d}B_i/\mathrm{d}t, (i = 1, 2) \tag{6}$$

where n is the number of coil turns, Φ_{ij} is the magnetic flux within a single turn, s_j is the effective cross-section area of a single turn, $B_1(t) = \mu_0 H(t)$ and $B_2(t) = \mu_0[H(t) + M(t)]$ are the magnetic induction intensity, and μ_0 is the magnetic permeability of the free space. The time-dependent fields at the primary coil read:

$$H(t) = H_{DC} + H_{AC}\cos\omega t = \mathrm{Re}[H_{DC} + H_{AC}\mathrm{e}^{\mathrm{i}\omega t}] \tag{7}$$

Whereas

$$M(t) = \mathrm{Re}[\chi H(t)] = [\chi'(H_{DC} + H_{AC}\cos\omega t) + \chi'' H_{AC}\sin\omega t] \tag{8}$$

which describes the MNP magnetization. Therefore, the recorded voltages at the secondary coil $V_1(t)$ and $V_2(t)$ are described by:

$$V_1(t) = \left(\mu_0 H_{AC}\omega \sum_{j=1}^{n} s_j\right)\sin\omega t = C_1 \sin\omega t \tag{9a}$$

$$V_2(t) = \left(\mu_0 H_{AC}\omega\sqrt{(1+\chi')^2 + (\chi'')^2}\sum_{j=1}^{n} s_j\right)\sin(\omega t - \alpha) = C_2\sin(\omega t - \alpha) \tag{9b}$$

where $\alpha = \arctan[\chi''/(1+\chi')]$ is the phase difference between $V_1(t)$ and $V_2(t)$. Parameters C_1, C_2 and α in equations (9*a*) and (9*b*) are obtained using the digital phase-sensitive detector (DPSD) algorithm. Then, susceptibility components (χ'' and χ') are extracted from:

$$\chi' = R/\sqrt{(\tan\alpha)^2 + 1} - 1 \text{ and } \chi'' = R\tan\alpha/\sqrt{(\tan\alpha)^2 + 1} \tag{10}$$

where $R = C_2/C_1$. In the present paper, the commercial water-based MF sample, purchased from Ocean NanoTech, LLC (Springdale, USA) is used to record data from which the temperature of liquid media can be extracted with high accuracy. This sample comprises magnetite nanoparticles surface-coated with first a monolayer of oleic acid and a second monolayer of amphiphilic polymer at a concentration of 5 mg-Fe/ml. The average core size of the as-suspended nanoparticles measured by transmission electron microscopy (TEM) is approximately 30 nm, whereas the hydrodynamic size assessed by dynamic light scattering (DLS) is approximately 8–10 nm larger than the core size, which shifts the effective relaxation time towards being Brownian-like (see figure 1) [15].

The susceptibility data obtained at room temperature, under an alternating sinusoidal field of 6 Oe amplitude and frequency in the range of 100 Hz to 10 kHz are shown in figure 3(a). Figure 3(b) collected correspondingly in the Cole–Cole plot indicates that the used sample follows the Debye model (see equation (1)) [17].

Once susceptibility components (χ'' and χ') are obtained, the relaxation time can be assessed using equation (2). Furthermore, the MNP-based magnetonanothermometer needs to be calibrated to operate remotely in a given temperature range and under weak applied fields using equation (5). In the present report calibration, parameters (A_1, A_2, A_3) were obtained using an optical-fiber temperature sensor purchased from HeQi Opto-Electronic Technology Co, Ltd (Xi' an, China).

4. Results and discussion

To achieve the approach for magnetonanothermometry, susceptibility data (χ'' and χ') were recorded at a selected amplitude ($H_{AC} = 6$ Oe) and frequency ($f = 5$ kHz) of an AC

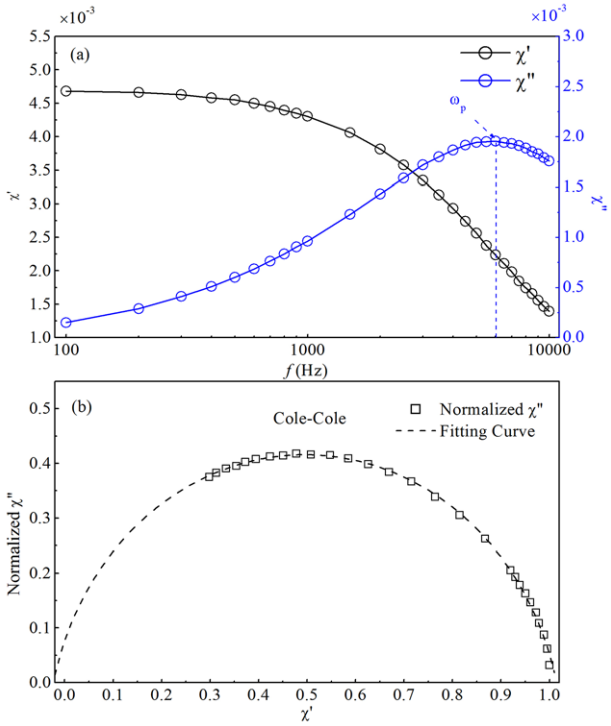

Figure 3. (a) Experimental data of χ' and χ'' at room temperature in the range of 100 Hz to 10 kHz and (b) the corresponding Cole–Cole plot, in which the black-dashed line is the curve fitting.

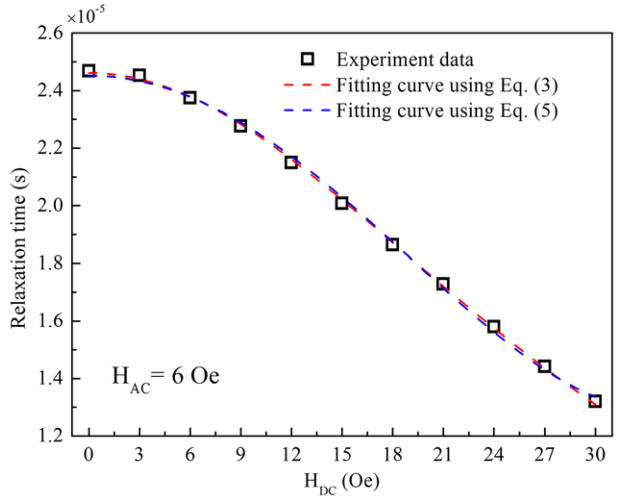

Figure 4. Effective relaxation time of MNPs at room temperature versus the DC field. The black square symbols represent the experimental data. The red-dashed line is the curve fitting using equation (3). The blue-dashed line is the curve fitting using equation (5).

applied field, as the strength of the DC field increases in a given range (below 30 Oe). When the strength of the applied magnetic field is sufficiently weak to allow the approximation proposed for the right-hand side of equation (3), the combination of driving frequency ($f = 5$ kHz) and average MNP size (30 nm average diameter) shifts the effective relaxation time towards being Brownian-like. The approximate model combining equations (2) and (5) was primarily valid by experiments, as shown in figure 4.

Figure 4 shows at room temperature the DC magnetic field dependence of the relaxation time obtained using equation (2), while using the experimental values of susceptibility components (χ'' and χ') obtained from the measuring system schematically presented in figure 2. An AC field with an amplitude of 6 Oe and a frequency of 5 kHz, as well as a DC field, was applied to excite the suspended MNPs. Our experimental results show that with an increase in the DC applied field from 0 to 30 Oe, the relaxation time decreases from 24.7 μs to 13.2 μs, as shown in figure 4. This has a good agreement with previous studies [18, 19], which demonstrates that our designed system allows an accurate measurement of AC susceptibility.

The symbols in figure 4 represent the experimental values whereas the red and blue dashed lines represent the best fitting based on equations (3) and (5), respectively. Inspection of the data fitting quality reveals that the approximation represented by equation (5) is excellent in the range of our experiment. At room temperature, we found the zero-field fitted relaxation time, $\tau_B(0)$, equals 2.46×10^{-5} and 2.45×10^{-5} s under equations (3) and (5), respectively. Alternatively, from the relationship $\tau = 1/\omega_P$ [15], the relaxation time can be estimated at a zero DC field via the peak position (ω_P) of an imaginary component of the AC susceptibility. Using the relationship, $\tau = 1/\omega_P$, and given the fact that $\chi''(\omega)$ peaks at approximately 6 kHz, we found $\tau_B(0)$ approximately equals 2.65×10^{-5} s at room temperature (see figure 3(a)), in very good agreement with the fitting values found from the data presented in figure 4. Therefore, this approximate approach is able to probe the temperature in a liquid environment.

The symbols in figure 5(a) show the susceptibility recorded at a DC applied field of 22.5 Oe under the usual operation conditions ($H_{AC} = 6$ Oe and $f = 5$ kHz), in which the in-phase and out-of-phase parts both decreased on increasing the temperature. Meanwhile, figure 5(b) shows the correlation between the temperature and relaxation time recorded in the range of 310 to 320 K at different DC applied fields (7.5, 15, 22.5, and 30 Oe). The data collected in figure 5(b) reveal a decrease in relaxation time as the temperature of the MF sample increases, as expected from equations (3) and (5). For data recording, the sample holder containing the SHP-30 MF sample was inserted in the secondary coil (see figure 2) and warmed up to slightly over 320 K. Then, the MF sample was cooled down naturally at a rate of approximately 7 K min^{-1} while recording the susceptibility data (χ'' and χ'). The magnetonanothermometer (surface-coated magnetite nanoparticle) was previously calibrated based on equation (5) (calibration parameters A_1, A_2, and A_3) using the commercial optical-fiber temperature sensor. For nanothermometer calibration and further operation, the MF sample viscosity (η) and the MNP's magnetic moment (m) were assumed to be constant in the operating range of the temperature and applied field. Moreover, we found that the calculated relaxation times in figure 5(b) (black solid lines) are effective based on equation (5).

Figure 6(a) shows the temperature error associated with the data presented in figure 6(b), whereas figure 6(b) shows the corresponding standard deviations for each employed DC applied field. We found temperature errors below 0.3 K with a maximum standard deviation of around 0.1 K. The increase in

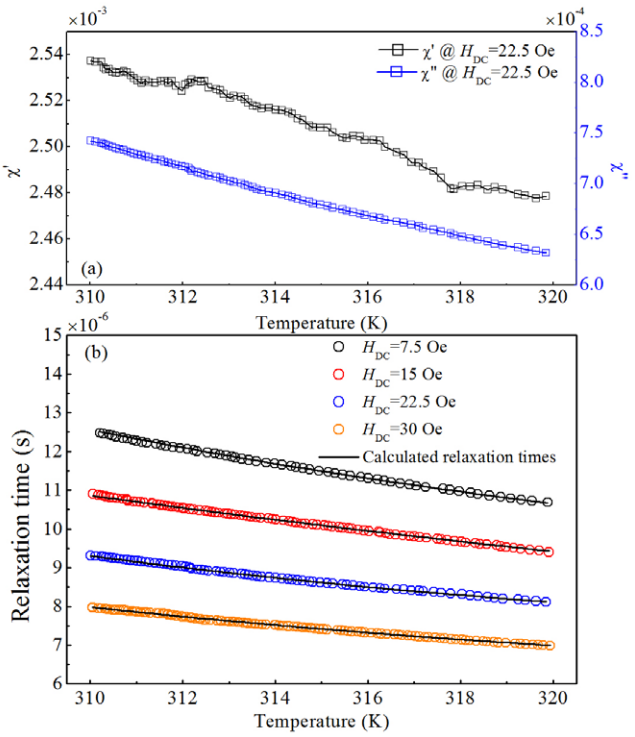

Figure 5. (a) Susceptibility recorded at $H_{DC} = 22.5$ Oe. (b) Data correlating measured relaxation time and calculated temperature at different DC applied fields (7.5, 15, 22.5, and 30 Oe). The temperature was calculated using equation (5) after performing calibration of parameters A_1, A_2, and A_3.

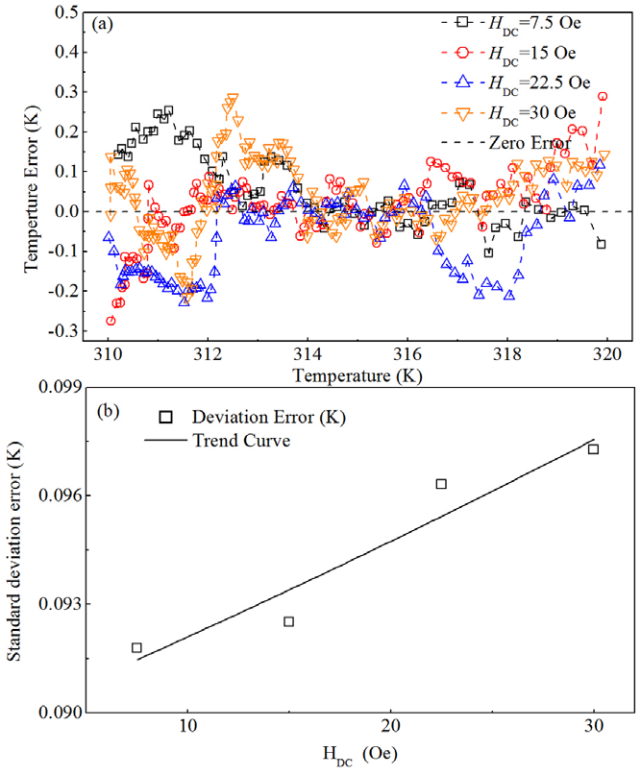

Figure 6. Experimental results of the temperature measurement accessed by our designed magnetonanothermometer. (a) shows the temperature error whereas (b) shows the standard deviations. The black solid line is only a guide for the eyes.

the standard deviation as the strength of the DC applied field increases is expected because of the truncation of the Taylor expansion represented by equation (5). The magnetonanothermometer introduced herein will be useful in fast and remote temperature monitoring while using intra–extracellular hyperthermia and thermal-assisted drug/gene delivery technologies. Moreover, the magnetonanothermometer could be integrated with MPI technology to incorporate temperature capability into imaging because the MNP probe size is within the same range for both technologies, whereas the AC applied magnetic field frequencies may be set differently [20].

5. Conclusion

In this study, we reported a new approach for fast and remote nanothermometry using AC susceptibility measurements of nanosized magnetic particles while dominated by the Brownian relaxation mechanism. The proposed magnetonanothermometer is meant to operate within a liquid environment under a combination of a low amplitude AC magnetic field in the kHz range and a weak DC magnetic bias field (up to 30 Oe). The magnetic sensor comprises a surface-coated magnetite nanoparticle (30 nm average core diameter) stably suspended as a commercial MF sample. Additionally, we introduce a simple, low cost, and accurate system to measure real and imaginary components of AC susceptibility from which the temperature can be extracted. After temperature calibration using a commercial optical fiber temperature sensor, the system and the approach presented here was tested in the 310 to 320 K temperature range, providing temperature errors lower than 0.3 K with standard deviations lower than 0.1 K. We envisage that the proposed approach is a promising tool to safely assist the use of intra–extracellular hyperthermia and thermally activated drug/gene delivery technologies.

Acknowledgments

This study was supported by projects 61571199 (NSFC), 2014AEA048 (HBSTD) and 61374014 (NSFC).

References

[1] Jordan A, Scholz R, Wust P, Fähling H and Felix R 1999 *J. Magn. Magn. Mater.* **201** 413–9
[2] Fortin J P, Gazeau F and Wilhelm C 2008 *Eur. Biophys. J.* **37** 223–8
[3] Kumar C S S R and Mohammad F 2011 *Adv. Drug Deliv. Rev.* **63** 789–808
[4] Sun C, Lee J S H and Zhang M Q 2008 *Adv. Drug Deliv. Rev.* **60** 1252–65
[5] Ducommun P, Rueux P A, Kadouri A, von Stockar U and Marison I W 2002 *Biotechnol. Bioeng.* **77** 838–42
[6] Johannsen M, Gneveckow U, Thiesen B, Taymoorian K, Cho C H, Waldöfner N, Scholz R, Jordan A, Loening S A and Wust P 2007 *Eur. Urol.* **52** 1653–62
[7] Soukup D, Moise S, Cespedes E, Dobson J and Telling N D 2015 *ACS Nano* **9** 231–40

[8] Perreard I M, Reeves D B, Zhang X, Kuehlert E, Forauer E R and Weaver J B 2014 *Phys. Med. Biol.* **59** 1109–19
[9] Rauwerdink A M, Hansen E W and Weaver J B 2009 *Phys. Med. Biol.* **54** L51–5
[10] Zhong J, Liu W Z, Jiang L, Yang M and Morais P C 2014 *Rev. Sci. Instrum.* **85** 094905-1–9
[11] Zhong J, Liu W Z, Kong L and Morais P C 2014 *Sci. Rep.* **4** 1–5
[12] Zhong J, Liu W Z, Du Z Z, de Morais P C, Xiang Q and Xie Q G 2012 *Nanotechnology* **23** 1–9
[13] Zhou M, Zhong J, Liu W Z, Du Z Z, Huang Z X, Yang M and Morais P C 2015 *IEEE Trans. Magn.* **51** 6101006-1–6
[14] Deissler R J, Wu Y and Martens M A 2014 *Med. Phys.* **41** 012301-1–13
[15] Rosensweig R E 2002 *J. Magn. Magn. Mater.* **252** 370–4
[16] Fannin P C, Marin C N and Couper C 2010 *J. Magn. Magn. Mater.* **322** 1677–81
[17] Fannin P C 2003 *J. Magn. Magn. Mater.* **258–259** 446–51
[18] Kalmykov Y P 2004 *Phys. Rev.* E **70** 051106-1–7
[19] Raĭkher Y L and Shliomis M I 1994 The effective field method in the orientational kinetics of magnetic fluids and liquid crystals *Advances in Chemical Physics: Relaxation Phenomena in Condensed Matter* vol 87, ed W Coffey (Hoboken, NJ: Wiley)
[20] Ishihara Y, Kuwabara T and Wadamori N 2011 *Electromagnetic Waves* ed V Zhurbenko (Rijeka: InTech) p 493